Original Article

Identification of a chemotherapy-associated gene signature for a risk model of prognosis in gastric adenocarcinoma through bioinformatics analysis

Yanping Shen[1], Ke Chen[1], Chijiang Gu[2]

[1]Department of Cancer Chemotherapy and Radiotherapy, The Affiliated People's Hospital of Ningbo University, Ningbo, China; [2]Department of Gastrointestinal Surgery, The Affiliated People's Hospital of Ningbo University, Ningbo, China

Contributions: (I) Conception and design: Y Shen; (II) Administrative support: K Chen; (III) Provision of study materials or patients: All authors; (IV) Collection and assembly of data: Y Shen; (V) Data analysis and interpretation: Y Shen, K Chen; (VI) Manuscript writing: All authors; (VII) Final approval of manuscript: All authors.

Correspondence to: Yanping Shen. Department of Cancer Chemotherapy and Radiotherapy, The Affiliated People's Hospital of Ningbo University, 251, Baizhang Eastern Road, Ningbo 315040, China. Email: shenyanping88@126.com.

Background: Over the past few years, the overall survival rate of patients with gastric adenocarcinoma who have received different chemotherapy regimens has increased. However, not all gastric cancer patients who receive chemotherapy have a longer survival. We need better predictive biomarkers. This study is to construct a new risk model of chemotherapy-associated genes in gastric adenocarcinoma (GA) for prognostication.

Methods: RNA-seq data and clinical information of GSE26901 (containing 44 chemotherapy samples and 65 patients without chemotherapy) in Gene Expression Omnibus (GEO) and stomach adenocarcinoma (STAD, containing 360 cancer tissue samples and 50 paired normal tissue samples) in The Cancer Genome Atlas (TCGA) were selected for screening differentially expressed genes (DEGs). Multivariate Cox regression was conducted to screen prognosis-associated genes and its link to patients' prognosis were screened by least absolute shrinkage and selection operator (LASSO) regression analysis. Based on the key genes, a risk scoring equation for the prognosis model was established, and constructed survival prognosis model. The model was tested for predictive ability through training set (TCGA datasets) and validation set (GSE84437). The correlations of the risk score with clinical pathological features, immune score and drug sensitivity score were evaluated.

Results: In total, 179 overlapping genes were obtained by screening DEGs. Univariate Cox analysis revealed 36 prognosis-related genes, and LASSO regression analysis revealed 8 key genes (*KCNJ2*, *GATA5*, *CLDN1*, *SERPINE1*, *FCER2*, *PMEPA1*, *TMEM37* and *CRTAC1*). Kaplan-Meier (K-M) analysis uncovered a relatively short overall survival time in the high-risk group. The model was verified to possess favourable predictive ability. In addition, the nomogram model were demonstrated good predictability with area under the curve (AUC) for 1–5 years in training set were 0.78, 0.78, 0.76, 0.79 and 0.81. The high-risk group was less likely to get benefits from immunotherapy and less sensitive to cisplatin.

Conclusions: According to the results of our training set and validation set, the risk model based on the eight chemotherapy-related gene signatures predicting prognosis has certain predictive accuracy in predicting the survival of GA patients which can be a promising prognostic parameter for GA. However, its efficacy remains to be proved in clinical practice.

Keywords: Chemotherapy treatment; gastric adenocarcinoma (GA); immunisation; prognosis; risk model

Submitted Aug 25, 2022. Accepted for publication Oct 10, 2022.

doi: 10.21037/jgo-22-872

View this article at: https://dx.doi.org/10.21037/jgo-22-872

Introduction

Digestive tract-associated tumours account for over half of the morbidity and mortality of all tumours, among which gastric adenocarcinoma (GA) is frequently seen worldwide (1). Thanks to continuous improvement in early diagnosis and surgical methods, and the application of chemotherapy (2), radiotherapy and biological agents (3), the overall level of GA treatment has achieved a significant improvement over the past few years (4). Surgery is still the leading treatment, including distal gastrectomy (5). For a long time, due to the late diagnosis of GA, the surgical outcome was poor, with a postoperative 5-year survival rate around 30% (6). Compared with non-screening or imaging, endoscopic screening can lower the risk of death from GA, and will not affect the incidence in Asian countries (7).

In addition to surgery, neoadjuvant chemotherapy (NACT) is an important therapy for digestive tract-associated tumours (8). And palliative treatment is the standard treatment for incurable advanced GA (9). A meta-analysis of individual patient data and a Cochrane systematic review verified the benefits of NACT (10), and 5-year follow-up data confirmed that NACT with S-1 after operation can prolong the overall survival (OS) as well as recurrence-free survival (RFS) of patients with stage II or III GA who underwent D2 gastrectomy (11). Moreover, 3-year follow-up data confirmed that postoperative NACT of S-1 combined with docetaxel can improve RFS and OS, and can be recommended as the standard for patients with stage III GA treated with D2 sandwich therapy (12). However, there is no consensus on which chemotherapy regimen is most effective in improving the OS and disease-free survival rates (13). Therefore, risk models based on genetics, diet, nutrition, living habits or occupational characteristics are being widely used in the prediction and prognosis of GA.

A large number of studies have identified a series of risk models that can be used to forecast GA patients' prognosis through bioinformatics methods. For instance, Zhou *et al.* (14) constructed a 4-genes-based prognosis prediction model by analysing and screening the differentially expressed genes (DEGs) of normal and GA tissues in The Cancer Genome Atlas (TCGA) as well as the Gene Expression Omnibus (GEO) and confirmed the validity of the model by data sets. However, the clinical heterogeneity of gastric cancer is mainly reflected in the inequality of treatment results. Its molecular mechanism remains unclear, including its molecular subtypes and related biomarkers have not been established, which cannot improve the prognosis and treatment of gastric cancer. Thus, in the presented study, we analyzed gene expression profiling data from gastric cancer patients through microarray technologies and uncovered potential prognostic subtypes, thereby identified the gene expression signature associated with prognosis and adjuvant chemotherapy response of gastric cancer. Meanwhile, the construction of a prognosis prediction model related to chemotherapy for GA has not been reported. Accordingly, we identified potential key chemotherapy-related genes of GA by bioinformatics methods, evaluated them and constructed a corresponding risk assessment model of GA and verified its prognostic value, with the goal of providing a reference for the treatment and improvement of prognosis of GA patients. We present the following article in accordance with the TRIPOD reporting checklist (available at https://jgo.amegroups.com/article/view/10.21037/jgo-22-872/rc).

Methods

Data source

From TCGA (https://portal.gdc.cancer.gov/), the clinicopathological parameters of stomach adenocarcinoma (STAD) samples and the RNA-seq of tumour tissue samples were downloaded. According to the integrity of the clinical sample data, as well as the matching with sequencing samples, duplicate and deleted samples and cases with missing clinical outcomes were screened. A total of 360 cancer tissue samples and 50 matched normal tissue samples were obtained. The GSE26901 data set was set as training set, downloaded from GEO (15), and was grouped according to the treatment with chemotherapy into 44 chemotherapy samples and 65 non-chemotherapy samples. In addition, the GSE84437 data set was downloaded as the verification set (16), and finally clinical phenotypic data on survival time and survival status of 110 tumour samples were obtained. The microarray data were normalized using the quantile normalization method in the Linear Models for Microarray Data package in the R language environment. The expression level of each gene was transformed into a log2 base before further analysis. The study was conducted in accordance with the Declaration of Helsinki (as revised in 2013).

DEG analysis

The gene expression matrix was analysed by limma software

package in R software. Using the Benjamini-Hochberg method, the P value was adjusted to the false discovery rate (FDR). With FDR <0.05 and |log2(Fold Change) |> log2(1.2) as the standard, DEGs were screened out. Using the R package ggplot2, a volcano map was drawn, and a Venn map revealed the overlapping genes.

Key genes screening and prognosis model construction

The survival package in the R software was used for univariate Cox regression analysis, with P<0.05 as the screening criterion. With the survminer package, the key genes were assigned to high or low expression groups based on the optimal cut-off value, and the corresponding survival curve was drawn. The least absolute shrinkage and selection operator (LASSO) regression algorithm was used to select the characteristics of key genes, and 10-fold cross-validation for determining the parameters. Using the Akaike Information Criterion (AIC), the selected genes underwent stepwise regression analysis for constructing a prognosis model. Kaplan-Meier (K-M) survival curves of the high- and low-risk groups were drawn by the survival package, and the timeROC package was utilised for drawing corresponding receiver operating characteristic (ROC) curves. The accuracy of the model in predicting prognosis was verified internally and externally.

Univariate and multivariate Cox regression analyses

Cox regression analysis was performed with the survival package, and a forest map was drawn by the forestplot package to report the P value, hazard ratio (HR) and 95% confidence interval (CI) of every variable. Based on the multivariate Cox proportional risk analysis, the RMS package was used to construct a nomogram for predicting the 1-, 2- and 3-year survival rates.

Immune score evaluation

The TIMER database (http://timer.comp-genomics.org/) was used to analyse the correlations of the expression of key genes in STAD with immune cell infiltration levels and immune cell markers. Using the CIBERSORT algorithm, the immune score was evaluated, and the correlation of key genes with immune checkpoint genes was analysed (17). The ESTIMATE algorithm was used to infer the immune score of each sample. The characteristic genes of 29 immune cells were extracted from a previous study (18), and the single-sample gene set enrichment analysis (ssGSEA) method was used to calculate the scores of the 29 immune cells. TIDE (http://tide.dfci.harvard.edu/) software was used for the evaluation of immunotherapy.

Gene mutation analysis

The SNV mutation of key genes was extracted by the maftools package, and the collinearity and mutual exclusion were analysed by the somaticInteractions function according to the mutation.

Statistical analysis

Statistical processing was carried out by R software v4.0.3 (R Foundation for Statistical Computing, 2020). DEGs were analysed by the unpaired Wilcox test, and the K-M method was used to evaluate survival. In order to compare the survival curves, the HR and log-rank P value in the K-M Plotter were calculated by the time series test. Pearson's correlation coefficient was used to analyse the correlation of genes with immune cells. We used the two-side test for all P values and P<0.05 suggested a notable difference.

Results

Screening of DEGs

Through differential expression analysis, 316 DEGs were obtained in the GSE26901 data set, including 222 differentially upregulated ones and 94 differentially down-regulated ones (*Figure 1A*). In the TCGA-STAD tumour tissues and normal tissues, 8,900 DEGs were screened, including 6694 differentially upregulated ones and 2206 differentially down-regulated ones (*Figure 1B*). Subsequently, 179 overlapping genes (Table S1) were obtained by intersecting the DEGs of the two data sets. We then screened out 36 genes associated with prognosis (Table S2) by conducting univariate Cox analysis of the 179 key genes.

Key genes screened by LASSO regression analysis

The 36 genes were further screened via LASSO regression for reducing the number of genes in the risk model. Firstly, the change track of every independent variable was

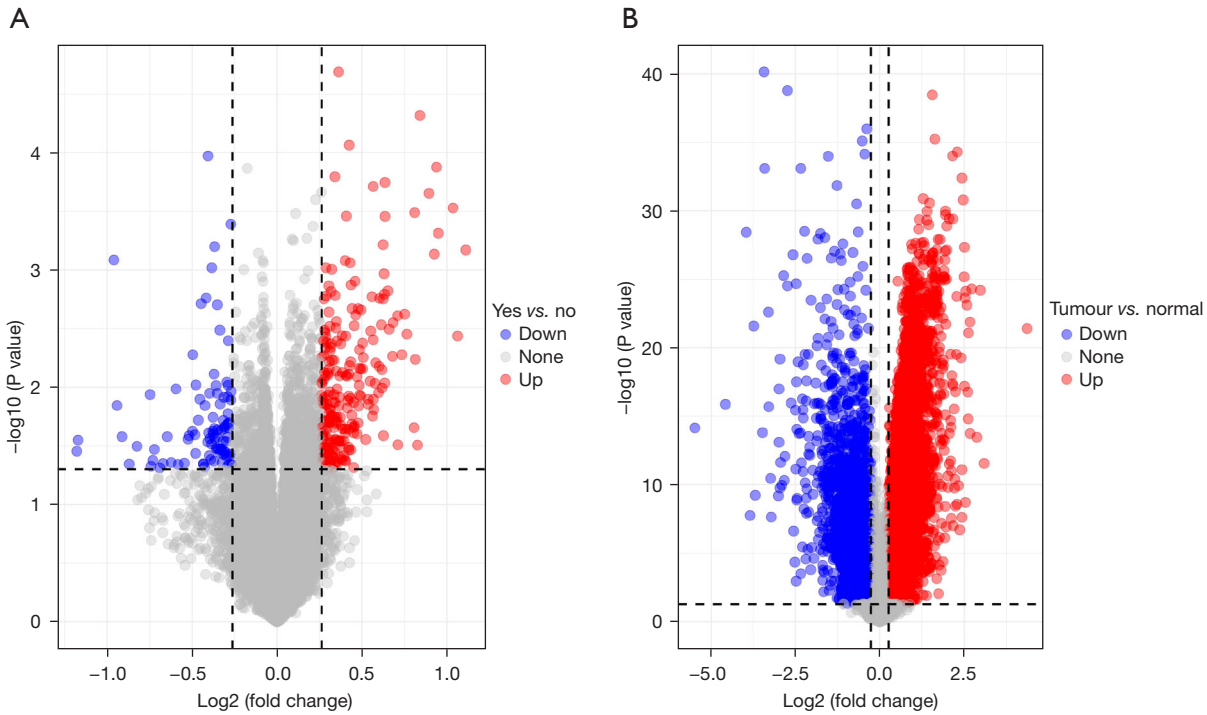

Figure 1 DEGs in (A) GSE26901 and (B) TCGA-STAD. DEG, differentially expressed gene; TCGA, The Cancer Genome Atlas; STAD, stomach adenocarcinoma.

analysed, as shown in *Figure 2A*. Accordingly, as the lambda increased gradually, the number of independent variable coefficients close to zero also increased gradually. Next, 10-fold cross-validation was used to build the model and analyse the CI under each lambda (*Figure 2B*). It can be seen from the figure that the model is optimal if lambda =0.0194, so 12 genes with lambda =0.0194 were adopted as the target genes. To further screen the key genes, we performed stepwise regression based on the AIC and used the stepAIC algorithm to optimise the model. Finally, 8 key genes were selected, namely *KCNJ2*, *GATA5*, *CLDN1*, *SERPINE1*, *FCER2*, *PMEPA1*, *TMEM37* and *CRTAC1*. Univariate Cox analysis showed the P value, risk coefficient, HR and CI of these 8 genes' expression and prognostic characteristics (*Figure 2C*).

Prognosis of key genes and mutation analysis

The K-M method was used to analyse the survival curves of the 8 key genes. According to the results, high *KCNJ2* expression was strongly associated with an unfavourable prognosis of STAD patients, while low expression of *GATA5*, *CLDN1*, *SERPINE1*, *FCER2*, *PMEPA1*, *TMEM37* and *CRTAC1* was strongly associated with a poor prognosis (*Figure 3*). Subsequently, the mutations of these 8 genes in STAD were evaluated (*Figure 4A*). The somatic interactions function analysis showed no collinearity and mutual exclusion among the 8 genes (*Figure 4B*). Additionally, only a few samples of the 8 genes were found to have copy number variation (CNV) mutations (*Figure 4C*). These results verified that these 8 key genes can stably help predict GA prognosis.

Correlation of key genes with immunity

For a deeper exploration of the correlation between key genes and immunity, we calculated the scores of 22 types of immune cells using the CIBERSORT algorithm, and then conducted an association analysis of immune cells and the 8 key genes by Pearson correlation analysis. According to the results, the expressions of *KCNJ2*, *FCER2* and *CRTAC1* were strongly associated with the scores of most immune cells (*Figure 5A*). Next, the immune score was calculated by the ESTIMATE method, and the correlation between immune score and the 8 key genes was also analysed by Pearson. According to the results, the expressions of *SERPNE1*,

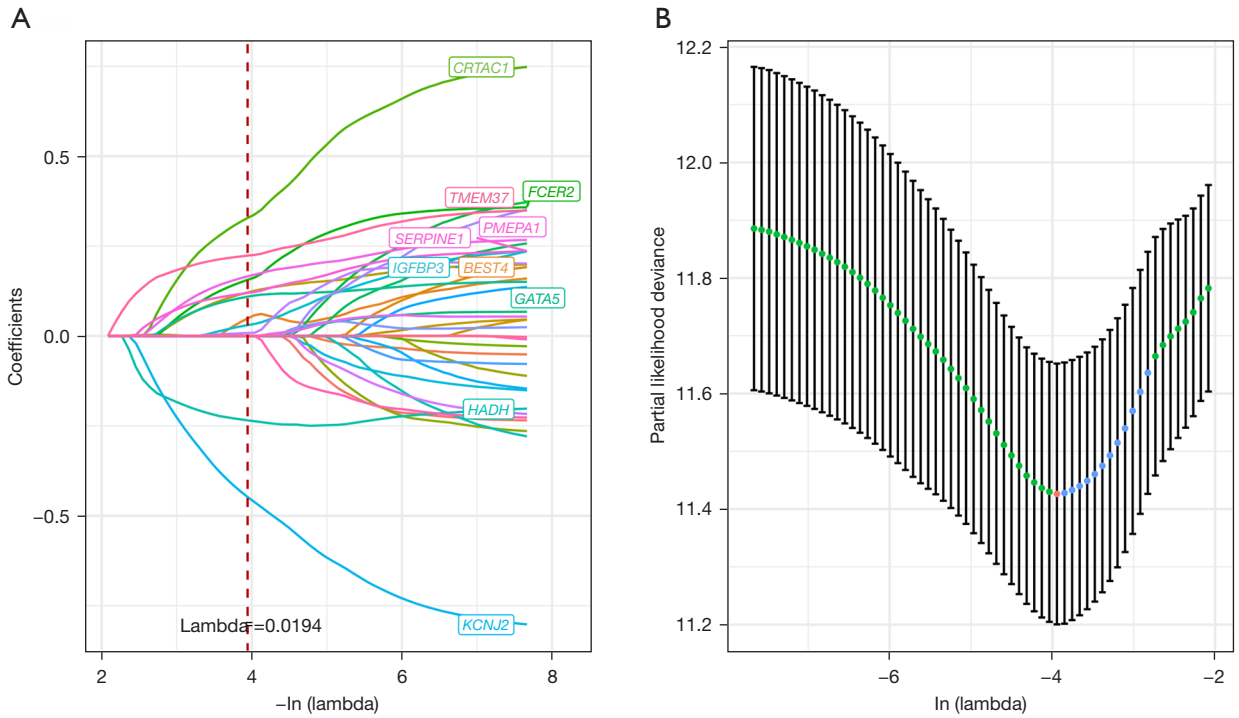

C

	P value	Hazard ratio (95% CI)
KCNJ2	0.002	0.570 (0.397–0.818)
GATA5	0.006	1.176 (1.047–1.321)
CLDN1	0.012	1.207 (1.042–1.397)
SERPINE1	0.003	1.229 (1.071–1.411)
FCER2	0.013	1.236 (1.046–1.459)
PMEPA1	0.005	1.244 (1.069–1.448)
TMEM37	<0.001	1.457 (1.228–1.729)
CRTAC1	0.004	1.569 (1.155–2.131)

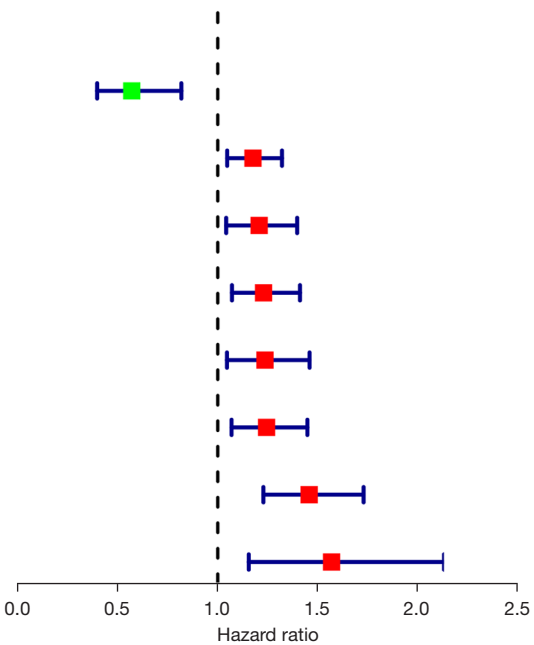

Figure 2 Screening of key genes by LASSO regression analysis. (A) The change track of every independent variable (horizontal axis: log value of the independent variable lambda; vertical axis: the coefficient of the independent variable). (B) Confidence interval under every lambda. (C) Forest map of 8 key genes. LASSO, least absolute shrinkage and selection operator.

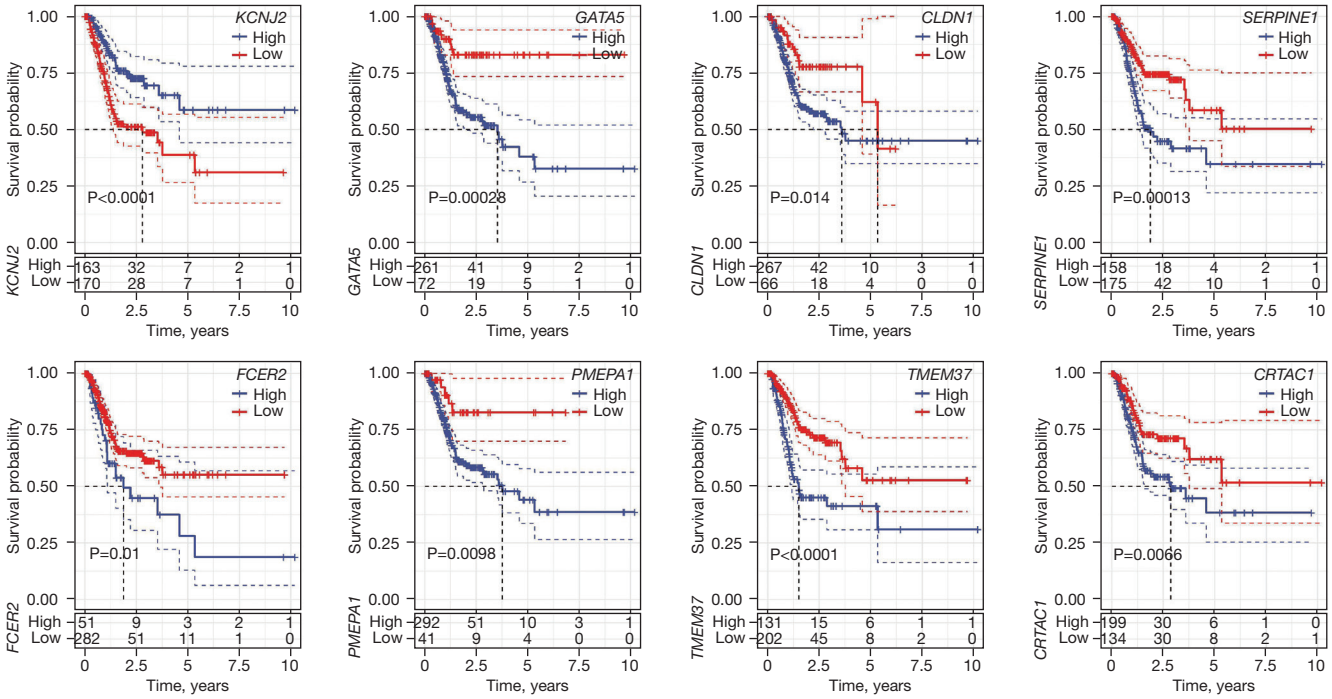

Figure 3 Survival analysis of 8 key genes in STAD. STAD, stomach adenocarcinoma.

FCER2 and *CRTAC1* were strongly linked to the immune score, matrix score and ESTIMATE score (*Figure 5B*). Additionally, we acquired the expression of immune checkpoint genes, and analysed their correlations with the 8 key genes by Pearson. According to the results, *SERPINE1*, *FCER2* and *TMEM37* were strongly linked to most immune checkpoint genes (*Figure 5C*). Moreover, we also calculated the immune cell score by the TIMER method, and found significant correlations between *FCER2* expression and the scores of 6 types of immune cell (*Figure 5D*). Finally, we extracted the characteristic genes of 29 immune cells, and calculated their scores by the ssGSEA method. The results indicated a strong association between the expressions of *SERPINE1* and *FCER2* and the scores of most immune cells (*Figure 5E*).

Construction of an 8-key-genes-based risk model for prognosis forecasting

With the TCGA data set as the training set, a risk model for prognosis forecasting based on the risk scores of the 8 key genes was constructed, and the samples were assigned to high- or low-risk group based on the median risk score. According to the results, the high-risk group had notably worse prognosis (*Figure 6A*). The ability of the model to predict the prognosis of patients in 1–5 years was calculated by the timeROC package, and the results showed that the model had an area under the curve (AUC) up to 0.7 (*Figure 6B*), indicating good ability in the TCGA data set for forecasting the patients' prognosis. The independent data set GSE84437 was used for verification, and K-M survival analysis uncovered a strong correlation of the high-risk group with poor prognosis, and also revealed the good predictive ability of the model for 1–5-year prognosis forecast (*Figure 6C,6D*). By analysing the diagnostic value of the 8 key genes and the combined risk model for treatment on the basis of the GSE26901 data set, the AUC of the risk model for prediction was found to be up to 0.7 (*Figure 6E*), but the AUC values of these eight genes for diagnosis were all less than 0.7 (*Figure 6F*). These results indirectly showed that the effect of the combined 8 genes to distinguish patients before and after treatment was better than that of each gene alone.

Clinicopathological characteristics and immune characteristics of different risk score groups

To test the relationship between risk scores and the

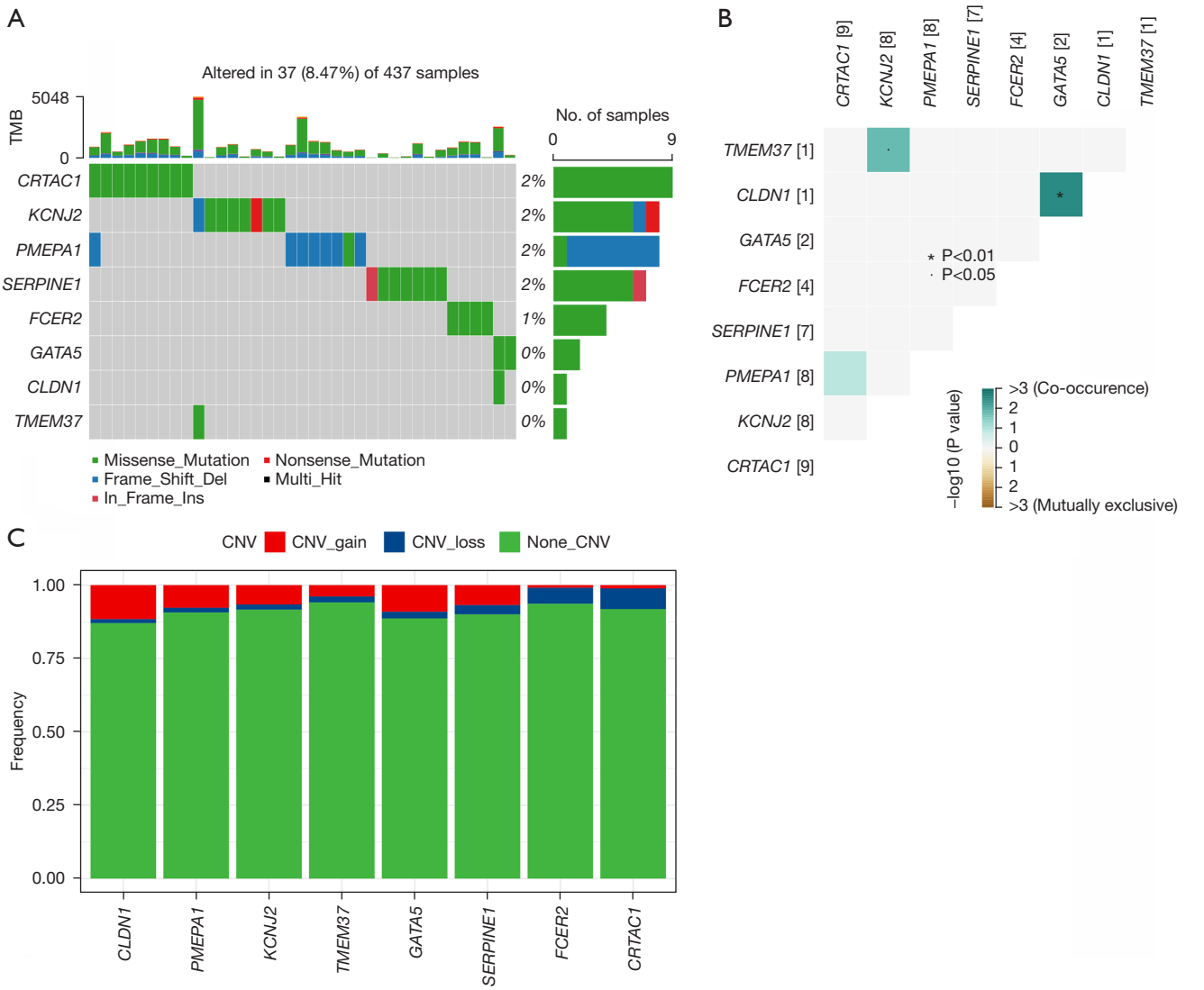

Figure 4 Mutation analysis of 8 key genes in STAD. (A) Waterfall map of mutations, (B) analysis of collinearity and mutual exclusion and (C) CNV mutation information. STAD, stomach adenocarcinoma; CNV, copy number variation.

clinical features of GA, we analysed risk scores between different TNM stages and clinical grades in the TCGA-STAD data set. The results showed that with increasing clinical grade, the risk score increased notably. In short, samples with a higher clinical grade had a higher risk score (*Figure* 7), and there was no notable difference in risk score between different sexes (P>0.05). For the purpose of clarifying differences in the immune microenvironment between different risk score groups, we compared the relative abundance of 22 immune cells in the high- and low-risk groups, and found notable differences between the risk score groups (*Figure 8A*). In addition, we also used ESTIMATE to evaluate immune cell infiltration, and found a notably lower immune score in the low-risk group, suggesting less immune cell infiltration in the low-risk group (*Figure 8B*). Moreover, we found different expressions of immune checkpoint genes between the groups (*Figure 8C*), and discovered strong correlations with the expression of most immune checkpoint genes. Further, we analysed the differences in immunotherapy among different molecular subtypes, and evaluated the potential clinical effects of immunotherapy in defined molecular subtypes

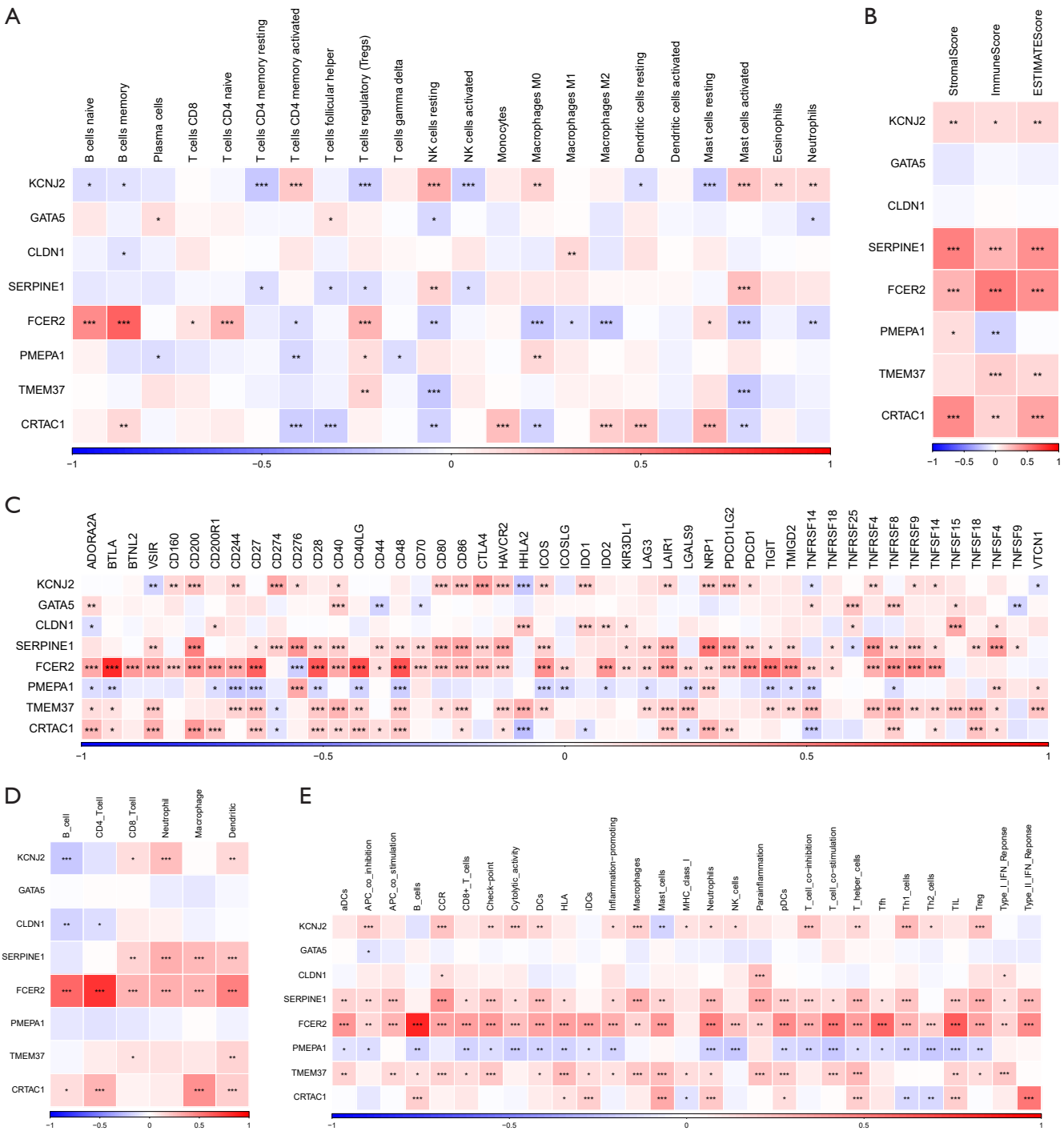

Figure 5 Correlation of key genes with immunity. (A) Association thermomap of 22 immune cell scores predicted by CIBERSORT and key genes. (B) Association thermomap between the immune score calculated by ESTIMATE and key genes. (C) Correlation thermomap between immune checkpoint genes and key genes. (D) Correlation thermomap between immune cell score calculated by TIMER and key genes. (E) Correlation thermomap between 29 immune cell scores calculated by the ssGSEA method and key genes. *, P<0.05; **, P<0.01; ***, P<0.001. ssGSEA, single-sample gene set enrichment analysis.

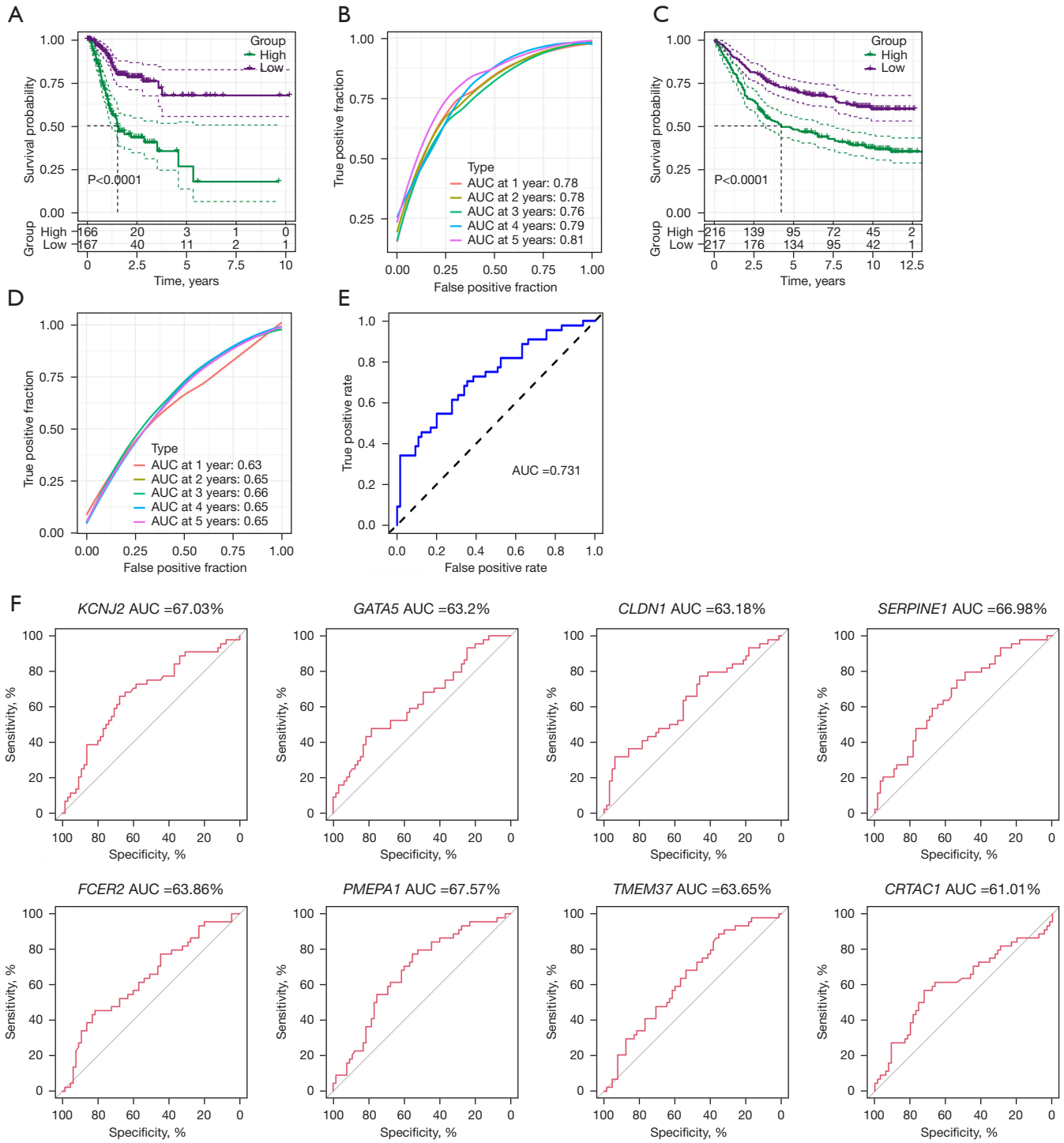

Figure 6 Risk model construction of the 8 key genes. (A) Survival analysis of high- and low-risk groups based on the TCGA data set. (B) ROC curve of the risk model in the TCGA data set. (C) Survival analysis of high- and low-risk groups based on the GSE84437 data set. (D) ROC curve of the risk model in the GSE84437 data set. (E) Diagnostic efficacy of the risk model in the GSE26901 data set. (F) Diagnostic efficacy of the 8 separate genes in the GSE26901 data set. AUC, area under the curve; TCGA, The Cancer Genome Atlas; ROC, receiver operating characteristic.

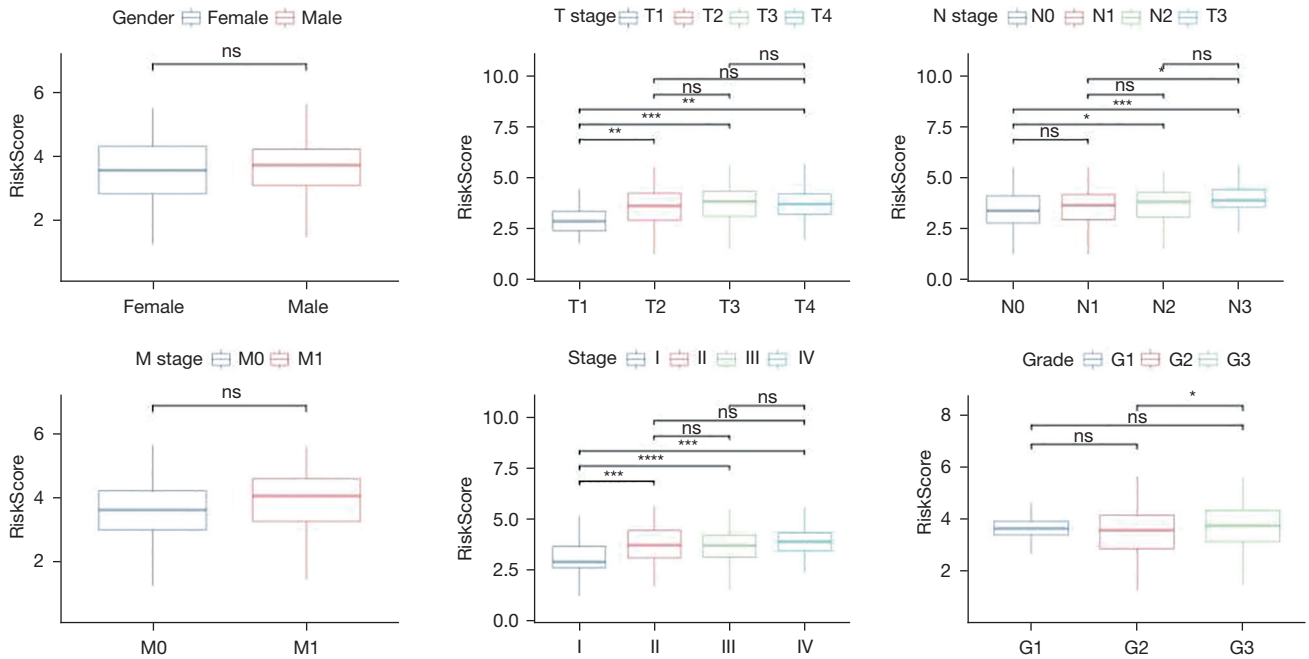

Figure 7 Clinicopathological features of the risk score groups. *, P<0.05; **, P<0.01; ***, P<0.001; ****, P<0.0001; ns, not significant.

using TIDE software. According to the results, the high-risk group had a notably higher TIDE score than the low-risk group in the TCGA cohort, suggesting that the high-risk group is more likely to escape immunity and less likely to benefit from immunotherapy (*Figure 8D*). We also analysed the response of different molecular subtypes in the TCGA cohort to cisplatin-based chemotherapy drugs, and found the high-risk group was more sensitive to these drugs than the low-risk group (*Figure 8E*). Overall, the results revealed differences in clinical phenotype and abnormalities in immune characteristics in the risk model based on the 8 key genes.

Univariate and multivariate Cox regression analyses

We analysed whether risk score was an independent prognostic factor of GA. Univariate and multivariate Cox regression analyses showed that sex and risk score may be independent prognostic factors of GA (*Figure 9A,9B*). We then generated a nomogram and used Cox regression to construct a model for forecasting 1-, 2- and 3-year OS (*Figure 9C*). The calibration results showed that in contrast to the ideal model, the 1, 2 and 3 years OS model had good predictability (*Figure 9D*), and the decision curve analysis showed that the nomogram was the optimal model (*Figure 9E*).

Discussion

NACT is a frequently used treatment for GA, which is often accompanied by tumour immune signals and microenvironment remodelling (19). However, clinical practice shows that more than a few GA patients gain no benefit from NACT because of the lack of biomarkers for patient selection and prognosis prediction (20). Therefore, to personalise the treatment it is essential to identify the patients who will benefit from NACT based on reliable prognostic and predictive factors. Although some clinical and tumour features can help identify patients with poor prognosis, they are not related to the treatment received (21-23). Therefore, it is imperative to identify the gene signature associated with treatment for predicting prognosis or the therapeutic effect.

In our study, TGCA-STAD data and GSE26901 data set were chosen, and 178 genes were identified using DEG analysis. A prediction model composed of 8 signature genes related to chemotherapy for GA was constructed via univariate Cox analysis and LASSO regression analysis. The

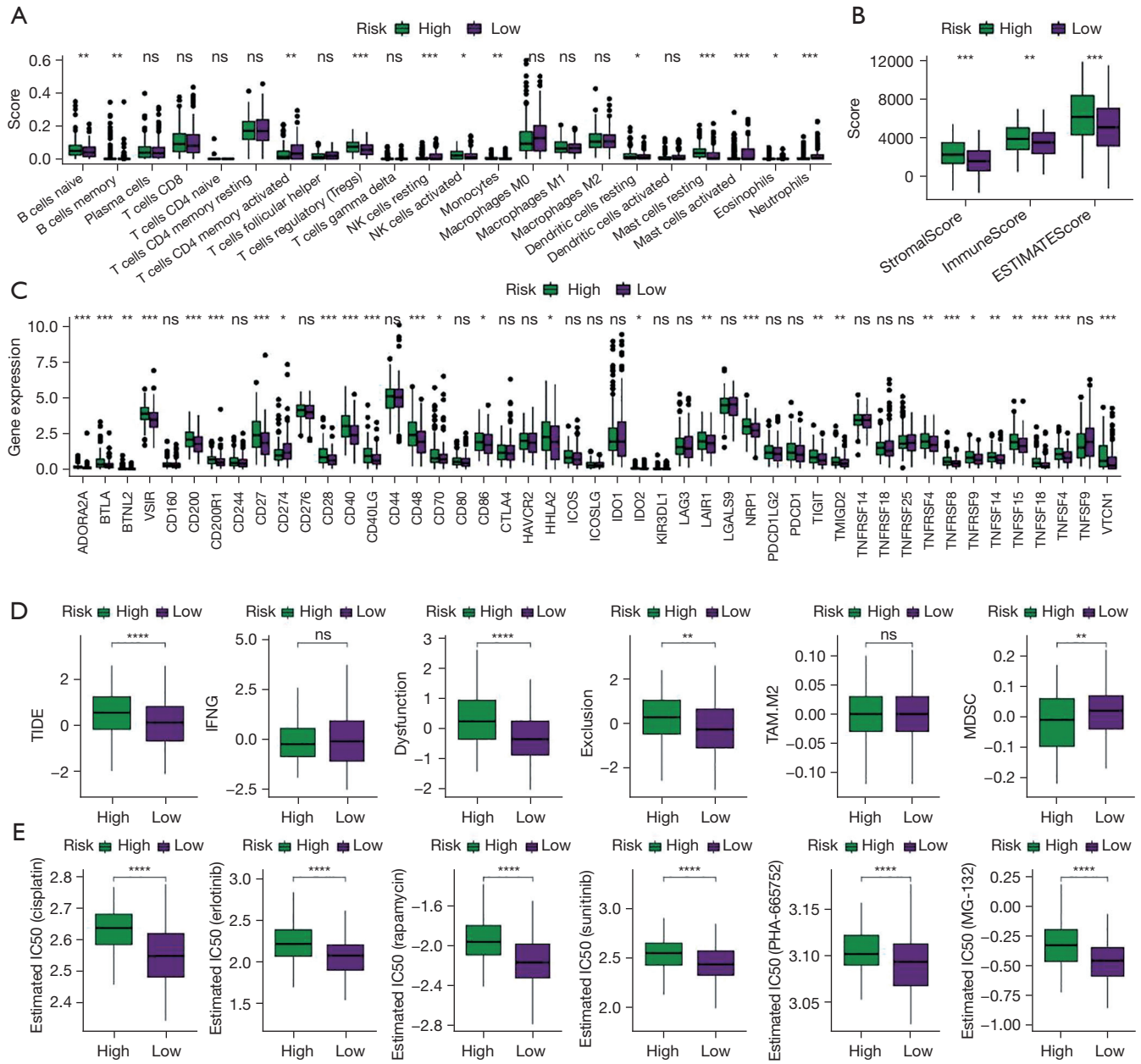

Figure 8 Immune characteristics of the risk score groups. Difference for (A) 22 immune cell scores and (B) ESTIMATE immune infiltration for the high- and low-risk score groups in the TCGA cohort. (C) Difference among immune checkpoints for the high- and low-risk score groups in the TCGA cohort. (D) Difference in the TIDE analysis results for the high- and low-risk score groups in the TCGA cohort. (E) Box plots of the estimated IC50 for drugs in TCGA-STAD. *, P<0.05; **, P<0.01; ***, P<0.001; ****, P<0.0001. ns, not significant. TIDE, tumor immune dysfunction and exclusion; IFNG, interferon γ; TAM, tumor-associated macrophage; MDSC, myeloid-derived suppressor cell; TCGA, The Cancer Genome Atlas; STAD, stomach adenocarcinoma.

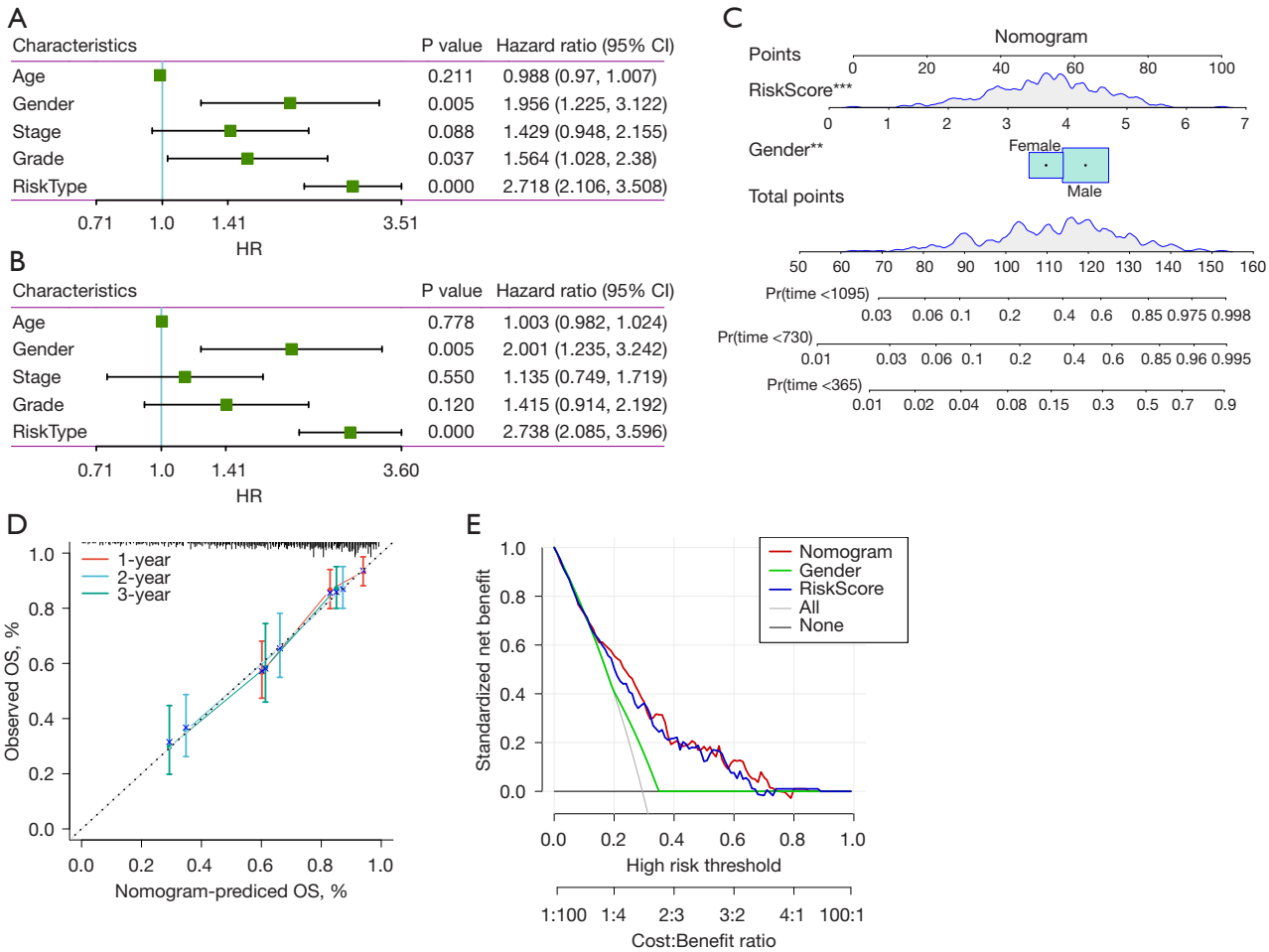

Figure 9 Clinical value of univariate and multivariate predictive risk models. (A) Univariate and (B) multivariate Cox analyses of risk score and clinicopathological features. (C) Nomogram. (D) 1-, 2- and 3-year survival calibration curves of the nomogram. (E) Decision curve analysis of the risk model. **, P<0.01; ***, P<0.001. OS, overall survival; CI, confidence interval.

model demonstrated high efficacy in forecasting the GA patients' prognosis within 1–5 years and could be used to effectively distinguish the curative effect in patients before and after chemotherapy.

The 8 signature genes related to chemotherapy comprise *KCNJ2*, *GATA5*, *CLDN1*, *SERPINE1*, *FCER2*, *PMEPA1*, *TMEM37* and *CRTAC1*. First, the correlation between these 8 genes and survival was analysed. According to the results, high KCNJ2 expression was strongly linked with an unfavourable prognosis, and patients with lower expression of the other 7 genes also had an unfavourable prognosis. The association of *KCNJ2* with tumour progression and prognosis has been confirmed by a previous study (24). Reportedly, in cases of small cell lung cancer, inhibiting the expression of *KCNJ2* promoted cell apoptosis, inhibited the cell cycle and enhanced the sensitivity of cancer cells to chemotherapeutic drugs (25). In addition, silencing *KCNJ2* expression can greatly weaken the invasion and metastasis of GA cells as well as epithelial–mesenchymal transformation (26). The correlations of these 8 key genes with immunity were also evaluated, and immune cells in GA cases were scored by different algorithms for correlation analysis of gene expression with immune score. Notably, the expression of *FCER2* was strongly linked to immune cell scores in the various algorithms. *FCER2* encodes the key molecule of B cell activation and growth. It is the receptor of immunoglobulin (Ig)E and is considered to be an ideal candidate gene for producing traits closely related to the IgE-mediated immune response (27,28). Moreover, FCER2 in urine has been identified as a biomarker that can be used

to improve eligibility for prostate biopsy and detect high-grade prostate cancer (29). The results of our study provide a starting point for its role in GA and immunity.

Finally, the relationship between the value of the 8-signature gene-based risk model for prognosis prediction of GA and clinical related characteristics was analysed. The risk model was found to have excellent 1–5-year prognostic efficacy, in both the training and validation sets. The risk model also demonstrated good diagnostic efficiency for predicting the chemotherapeutic effect of GA. In addition, the risk scores were grouped based on this risk model and their correlation with immune characteristics were analysed. The results revealed notable differences in some immune cell scores among the different risk score groups, and also revealed lower immune cell infiltration and a lower possibility of immune escape in the low-risk group. More and more evidences show that the tumour microenvironment, including tumour-infiltrating immune cells, supports the growth and development of cancer, and further promotes invasion, metastasis and sensitivity to drug therapy (30,31). Immune escape surveillance, in which the host immune system recognises and destroys cancer cells, is a sign of biological ability (32) and has been reported in both animal and human cancer patients, which supports the hypothesis that the immune escape of cancer cells is a crucial step in tumour development (33). There is an immunogenic interaction between tumour and host, and tumour immune escape recognition often determines the clinical course of the disease (34). Therefore, we believe that our risk model will be helpful in identifying tumour immune escape and can be used to determine the clinical course of the disease. Moreover, the results showed that as clinical grade increases, the risk score increases notably. Therefore, this risk model can be used to predict the chemotherapeutic effect and prognosis of GA patients, and can be used to study changes in the tumour microenvironment during the development of GA.

Conclusions

We constructed an effective and accurate STAD prognosis prediction model based on 8 chemotherapy-related signature genes, which demonstrated good predictability. According to the risk score, it is able to strongly distinguish high-risk from low-risk patients, and can be used to identify the clinical course and chemotherapeutic effect of GA patients. However, this study also had some limitations. It mainly depended on bioinformatics analysis, so the results need to be verified by a series of biological experiments, and the potential biological mechanisms and pathways associated with these 8 genes need further study.

Acknowledgments

Funding: This study was supported by Fund of Ningbo Yinzhou Science and Technology Bureau (No. 2017-110).

Footnote

Reporting Checklist: The authors have completed the TRIPOD reporting checklist. Available at https://jgo.amegroups.com/article/view/10.21037/jgo-22-872/rc

Conflicts of Interest: All authors have completed the ICMJE uniform disclosure form (available at https://jgo.amegroups.com/article/view/10.21037/jgo-22-872/coif). The authors have no conflicts of interest to declare.

Ethical Statement: The authors are accountable for all aspects of the work in ensuring that questions related to the accuracy or integrity of any part of the work are appropriately investigated and resolved. The study was conducted in accordance with the Declaration of Helsinki (as revised in 2013).

References

1. Deng W, Jin L, Zhuo H, et al. Alcohol consumption and risk of stomach cancer: A meta-analysis. Chem Biol Interact 2021;336:109365.
2. Clark PI, Slevin ML. Chemotherapy for stomach cancer. Br Med J (Clin Res Ed) 1987;295:870-1.
3. Tey J, Soon YY, Koh WY, et al. Palliative radiotherapy for gastric cancer: a systematic review and meta-analysis. Oncotarget 2017;8:25797-805.
4. Kelly RJ, Ajani JA, Kuzdzal J, et al. Adjuvant Nivolumab

in Resected Esophageal or Gastroesophageal Junction Cancer. N Engl J Med 2021;384:1191-203.
5. Lu J, Zheng CH, Xu BB, et al. Assessment of Robotic Versus Laparoscopic Distal Gastrectomy for Gastric Cancer: A Randomized Controlled Trial. Ann Surg 2021;273:858-67.
6. Yu J, Huang C, Sun Y, et al. Effect of Laparoscopic vs Open Distal Gastrectomy on 3-Year Disease-Free Survival in Patients With Locally Advanced Gastric Cancer: The CLASS-01 Randomized Clinical Trial. JAMA 2019;321:1983-92.
7. Zhang X, Li M, Chen S, et al. Endoscopic Screening in Asian Countries Is Associated With Reduced Gastric Cancer Mortality: A Meta-analysis and Systematic Review. Gastroenterology 2018;155:347-354.e9.
8. Park SH, Lim DH, Sohn TS, et al. A randomized phase III trial comparing adjuvant single-agent S1, S-1 with oxaliplatin, and postoperative chemoradiation with S-1 and oxaliplatin in patients with node-positive gastric cancer after D2 resection: the ARTIST 2 trial☆. Ann Oncol 2021;32:368-74.
9. Fujitani K, Yang HK, Mizusawa J, et al. Gastrectomy plus chemotherapy versus chemotherapy alone for advanced gastric cancer with a single non-curable factor (REGATTA): a phase 3, randomised controlled trial. Lancet Oncol 2016;17:309-18.
10. Ge L, Hou L, Yang Q, et al. A systematic review and network meta-analysis protocol of adjuvant chemotherapy regimens for resected gastric cancer. Medicine (Baltimore) 2019;98:e14478.
11. Sasako M, Sakuramoto S, Katai H, et al. Five-year outcomes of a randomized phase III trial comparing adjuvant chemotherapy with S-1 versus surgery alone in stage II or III gastric cancer. J Clin Oncol 2011;29:4387-93.
12. Kakeji Y, Yoshida K, Kodera Y, et al. Three-year outcomes of a randomized phase III trial comparing adjuvant chemotherapy with S-1 plus docetaxel versus S-1 alone in stage III gastric cancer: JACCRO GC-07. Gastric Cancer 2022;25:188-96.
13. Zhang YW, Zhang YL, Pan H, et al. Chemotherapy for patients with gastric cancer after complete resection: a network meta-analysis. World J Gastroenterol 2014;20:584-92.
14. Zhou L, Li SH, Wu Y, et al. Establishment of a prognostic model of four genes in gastric cancer based on multiple data sets. Cancer Med 2021;10:3309-22.
15. Oh SC, Sohn BH, Cheong JH, et al. Clinical and genomic landscape of gastric cancer with a mesenchymal phenotype. Nat Commun 2018;9:1777.
16. Yoon SJ, Park J, Shin Y, et al. Deconvolution of diffuse gastric cancer and the suppression of CD34 on the BALB/c nude mice model. BMC Cancer 2020;20:314.
17. Danilova L, Ho WJ, Zhu Q, et al. Programmed Cell Death Ligand-1 (PD-L1) and CD8 Expression Profiling Identify an Immunologic Subtype of Pancreatic Ductal Adenocarcinomas with Favorable Survival. Cancer Immunol Res 2019;7:886-95.
18. Bindea G, Mlecnik B, Tosolini M, et al. Spatiotemporal dynamics of intratumoral immune cells reveal the immune landscape in human cancer. Immunity 2013;39:782-95.
19. Li Z, Gao X, Peng X, et al. Multi-omics characterization of molecular features of gastric cancer correlated with response to neoadjuvant chemotherapy. Sci Adv 2020;6:eaay4211.
20. Li Z, Jia Y, Zhu H, et al. Tumor mutation burden is correlated with response and prognosis in microsatellite-stable (MSS) gastric cancer patients undergoing neoadjuvant chemotherapy. Gastric Cancer 2021;24:1342-54.
21. van den Boorn HG, Engelhardt EG, van Kleef J, et al. Prediction models for patients with esophageal or gastric cancer: A systematic review and meta-analysis. PLoS One 2018;13:e0192310.
22. Sohn BH, Hwang JE, Jang HJ, et al. Clinical Significance of Four Molecular Subtypes of Gastric Cancer Identified by The Cancer Genome Atlas Project. Clin Cancer Res 2017;23:4441-9.
23. Shao W, Yang Z, Fu Y, et al. The Pyroptosis-Related Signature Predicts Prognosis and Indicates Immune Microenvironment Infiltration in Gastric Cancer. Front Cell Dev Biol 2021;9:676485.
24. Valdora FF, Freier C, Seyler N, et al. Kcnj2 comprises a marker of poor prognosis and a therapeutic target in non-wnt/non-shh medulloblastoma. Cancer Res 2012;72:1424-24.
25. Liu H, Huang J, Peng J, et al. Upregulation of the inwardly rectifying potassium channel Kir2.1 (KCNJ2) modulates multidrug resistance of small-cell lung cancer under the regulation of miR-7 and the Ras/MAPK pathway. Mol Cancer 2015;14:59.
26. Ji CD, Wang YX, Xiang DF, et al. Kir2.1 Interaction with Stk38 Promotes Invasion and Metastasis of Human Gastric Cancer by Enhancing MEKK2-MEK1/2-ERK1/2 Signaling. Cancer Res 2018;78:3041-53.
27. Laitinen T, Ollikainen V, Lázaro C, et al. Association study of the chromosomal region containing the FCER2 gene

suggests it has a regulatory role in atopic disorders. Am J Respir Crit Care Med 2000;161:700-6.
28. Shen M, Vermeulen R, Rajaraman P, et al. Polymorphisms in innate immunity genes and lung cancer risk in Xuanwei, China. Environ Mol Mutagen 2009;50:285-90.
29. Alijaj N, Pavlovic B, Martel P, et al. Identification of Urine Biomarkers to Improve Eligibility for Prostate Biopsy and Detect High-Grade Prostate Cancer. Cancers (Basel) 2022;14:1135.
30. Steven A, Seliger B. The Role of Immune Escape and Immune Cell Infiltration in Breast Cancer. Breast Care (Basel) 2018;13:16-21.
31. Lin Y, Pan X, Zhao L, et al. Immune cell infiltration signatures identified molecular subtypes and underlying mechanisms in gastric cancer. NPJ Genom Med 2021;6:83.
32. Hanahan D, Weinberg RA. Hallmarks of cancer: the next generation. Cell 2011;144:646-74.
33. Klein G, Klein E. Surveillance against tumors--is it mainly immunological? Immunol Lett 2005;100:29-33.
34. Hoenicke L, Zender L. Immune surveillance of senescent cells--biological significance in cancer- and non-cancer pathologies. Carcinogenesis 2012;33:1123-6.

(English Language Editor: K. Brown)

Cite this article as: Shen Y, Chen K, Gu C. Identification of a chemotherapy-associated gene signature for a risk model of prognosis in gastric adenocarcinoma through bioinformatics analysis. J Gastrointest Oncol 2022;13(5):2219-2233. doi: 10.21037/jgo-22-872

Table S1 179 genes associated with tumorigenesis and chemotherapy treatment

Gene					
ENC1	*PMEPA1*	*MTTP*	*CRTAC1*	*TESK2*	*POU2AF1*
SERPINH1	*ANGPT2*	*PTK7*	*FOXC1*	*DPYSL2*	*PTGER4*
SOX4	*IER5L*	*GTF3A*	*DIO2*	*HIST3H2A*	*IFITM2*
CTHRC1	*SLC1A5*	*BEST4*	*NID2*	*ADH4*	*BRSK1*
COL1A1	*COL1A2*	*RCN3*	*MIF*	*LRRC32*	*FSTL1*
BGN	*RAB15*	*SFRP4*	*MMP10*	*TM4SF18*	*ITGBL1*
PUS7	*FAP*	*DISP1*	*COL4A2*	*FSTL3*	*LDB2*
CST1	*SPARC*	*IFITM3*	*MSX1*	*BMPR2*	*SLC4A2*
CLDN1	*SERPINE1*	*SIDT2*	*AGT*	*CDH5*	*YAP1*
COL4A1	*CPXM1*	*CDK6*	*TM6SF2*	*LUM*	*PLVAP*
ESM1	*COL12A1*	*STC2*	*ADAMTSL2*	*ACE2*	*CTSK*
OTOP3	*NOTCH3*	*NUAK1*	*NOS3*	*CAT*	*CALCRL*
COL5A2	*THBS2*	*NOX4*	*OXTR*	*MCOLN2*	*THBS1*
PTPN12	*SLC25A34*	*APOB*	*GDPD2*	*CREB3L3*	*PCDH18*
MS4A10	*HAPLN3*	*CDH11*	*COMP*	*TGFBI*	*LAMC1*
EPHB4	*PDGFRB*	*PXDN*	*TNNC1*	*IGFBP7*	*EDNRA*
CCT2	*SLC39A1*	*COL7A1*	*PLS3*	*SH3PXD2B*	*PCOLCE*
MMP11	*FNDC1*	*COL6A3*	*ENG*	*SULT1B1*	*SLC6A8*
PLAU	*MXRA5*	*C1orf198*	*CYB5A*	*GJA4*	*PLEKHA4*
HPGD	*OLFML2B*	*LZTS1*	*TBX10*	*TMEM147*	*TMEM119*
GKN2	*VCAN*	*COL8A1*	*WNT5A*	*UBTD1*	*FCER2*
DNASE1L3	*CHSY3*	*FZD2*	*HES4*	*SRPX2*	*SLC7A9*
FOXS1	*ALDOC*	*FSCN1*	*EMP1*	*COL15A1*	*CHP2*
TIMP1	*LAMB1*	*STC1*	*NKD2*	*KCNJ2*	*GLRX*
COL10A1	*COL5A1*	*SALL4*	*ICAM3*	*CLC*	*GREM1*
COL3A1	*GPR4*	*SLC2A5*	*ADAMTS9*	*TMEM37*	*PTP4A3*
THY1	*IGFBP3*	*SPON2*	*GATA5*	*INHBB*	*NOTUM*
SULF1	*GGH*	*CHSY1*	*RBKS*	*NNMT*	*MGP*
GKN1	*HADH*	*HEYL*	*SLC28A2*	*DDAH2*	*AEBP1*
CALU	*LEF1*	*NETO2*	*PSD4*	*CLEC11A*	

https://dx.doi.org/10.21037/jgo-22-872

Table S2 Univariate COX analysis of 179 genes

Gene	P value	HR	Low 95% CI	High 95% CI
ENC1	0.99111589	0.99875337	0.80186261	1.24398903
SERPINH1	0.22755603	1.18259297	0.90059922	1.55288403
SOX4	0.21682884	1.14317825	0.92445665	1.41364823
CTHRC1	0.06439859	1.14994202	0.99168313	1.33345683
COL1A1	0.14113844	1.10628761	0.96703142	1.26559722
BGN	0.02458247	1.19629151	1.02322296	1.398633
PUS7	0.18835413	0.81173631	0.59490631	1.10759598
CST1	0.16196605	1.06508645	0.97500167	1.16349457
CLDN1	0.01199434	1.20680662	1.04219393	1.3974196
COL4A1	0.8997047	1.01402903	0.81650842	1.25933162
ESM1	0.26669952	0.88111792	0.70475725	1.10161163
OTOP3	0.1500691	1.19193524	0.93845801	1.51387659
COL5A2	0.17538441	1.13246851	0.94598678	1.35571126
PTPN12	0.14797737	1.32137146	0.90586591	1.92746245
MS4A10	0.19343964	1.31677451	0.86974817	1.99355992
EPHB4	0.74994713	1.04751321	0.7873805	1.39358789
CCT2	0.59957507	0.92582984	0.69436203	1.23445818
MMP11	0.04560896	1.1292835	1.00237674	1.27225741
PLAU	0.90991239	0.98987489	0.82989378	1.18069602
HPGD	0.85078262	1.01394869	0.87768231	1.17137139
GKN2	0.76811309	1.01179203	0.93593857	1.09379306
DNASE1L3	0.61174291	1.07689075	0.80899556	1.43349821
FOXS1	0.00492406	1.35431427	1.09625021	1.6731282
TIMP1	0.12462071	1.15947491	0.95994152	1.40048332
COL10A1	0.04679532	1.12334546	1.00165019	1.25982607
COL3A1	0.09194755	1.12965297	0.98032035	1.30173348
THY1	0.38254473	1.08602177	0.90239731	1.30701108
SULF1	0.18239515	1.09665493	0.95757293	1.25593779
GKN1	0.68233004	1.01251814	0.95395993	1.0746709
CALU	0.85595233	1.03060709	0.74426402	1.42711585
PMEPA1	0.00471702	1.24448782	1.06931167	1.44836158
ANGPT2	0.82197046	0.96756935	0.72604889	1.28943168
IER5L	0.47384399	0.92970461	0.76159145	1.13492696
SLC1A5	0.26640976	0.89499637	0.73596176	1.08839691
COL1A2	0.14136728	1.11607187	0.96412833	1.29196123

Table S2 (*continued*)

https://dx.doi.org/10.21037/jgo-22-872

Table S2 (*continued*)

Gene	P value	HR	Low 95% CI	High 95% CI
RAB15	0.35979063	0.90865967	0.74023488	1.11540596
FAP	0.18326906	1.16557549	0.9301188	1.4606373
SPARC	0.10343479	1.16154405	0.96997171	1.3909525
SERPINE1	0.00329855	1.22937057	1.07118353	1.41091789
CPXM1	0.25138562	1.10385675	0.93236069	1.30689736
COL12A1	0.57951883	1.04752922	0.88885889	1.23452381
NOTCH3	0.01892879	1.30502063	1.0448723	1.62993969
THBS2	0.13152978	1.10163913	0.97141287	1.24932335
SLC25A34	0.61684441	0.88396712	0.54526423	1.43306277
HAPLN3	0.26281808	1.13261338	0.91079321	1.408457
PDGFRB	0.07963604	1.18781495	0.97986332	1.43989913
SLC39A1	0.99599399	1.00087331	0.71184787	1.40724924
FNDC1	0.03728189	1.13990435	1.00774439	1.28939634
MXRA5	0.52321801	1.0538811	0.89705249	1.23812752
OLFML2B	0.12485892	1.14043195	0.96424159	1.34881656
VCAN	0.0153998	1.24176816	1.04223602	1.47949998
CHSY3	0.68431318	1.10033913	0.69397752	1.74464758
ALDOC	0.82167913	1.02549225	0.82387999	1.27644119
LAMB1	0.2491859	1.1563023	0.9032231	1.4802932
COL5A1	0.13480875	1.13569553	0.9612414	1.34181105
GPR4	0.92844051	1.014704	0.73788375	1.39537455
IGFBP3	0.03061089	1.20770241	1.01779964	1.43303755
GGH	0.08818348	0.87324875	0.74726751	1.02046906
HADH	0.00042848	0.5355556	0.37833971	0.75810122
LEF1	0.07506805	1.23530778	0.97886763	1.55892918
MTTP	0.49222994	1.06630827	0.88778553	1.28072973
PTK7	0.44185483	1.06857402	0.90239353	1.26535751
GTF3A	0.75618693	0.95339285	0.7053859	1.28859668
BEST4	0.01353853	1.94266432	1.14679338	3.29086715
RCN3	0.27674034	1.10830926	0.92083687	1.33394899
SFRP4	0.06198796	1.09694976	0.99537104	1.2088947
DISP1	0.23839965	1.30407131	0.83873417	2.02758162
IFITM3	0.96082495	1.00535846	0.81228603	1.2443223
SIDT2	0.53792434	1.10543424	0.80354737	1.52073781

Table S2 (*continued*)

https://dx.doi.org/10.21037/jgo-22-872

Table S2 (*continued*)

Gene	P value	HR	Low 95% CI	High 95% CI
CDK6	0.83728564	0.98093904	0.81634876	1.17871362
STC2	0.77378977	0.96081563	0.73157747	1.26188507
NUAK1	0.00413961	1.60273791	1.16098961	2.2125683
NOX4	0.03033385	1.68222377	1.05065158	2.69344935
APOB	0.07246566	1.13321352	0.98866157	1.29890038
CDH11	0.06761862	1.20780076	0.98641257	1.47887681
PXDN	0.54083748	1.0756884	0.85139991	1.35906232
COL7A1	0.40572109	1.07918695	0.90173333	1.29156197
COL6A3	0.29952301	1.08962379	0.92651754	1.28144363
C1orf198	0.46686196	1.14324333	0.79712618	1.6396467
LZTS1	0.01810553	1.36711863	1.05483576	1.77185247
COL8A1	0.02300867	1.19012635	1.02428063	1.38282488
FZD2	0.003368	1.34195585	1.10242301	1.63353403
FSCN1	0.07202358	1.16284343	0.9865891	1.37058563
STC1	0.2216665	1.13247191	0.92764246	1.38252903
SALL4	0.25310759	1.10357528	0.93195823	1.30679504
SLC2A5	0.83673339	1.03883501	0.72305654	1.49252254
SPON2	0.28546586	1.11261082	0.9147555	1.35326088
CHSY1	0.529566	1.12222266	0.7833404	1.60770936
HEYL	0.01585271	1.25676133	1.04378429	1.51319487
NETO2	0.87877365	0.98059006	0.76225451	1.26146433
CRTAC1	0.00392203	1.5690971	1.15532245	2.13106367
FOXC1	0.77142449	0.97472839	0.82013626	1.15846048
DIO2	0.37901001	1.08992675	0.89966017	1.32043227
NID2	0.43900242	1.09475533	0.87044375	1.37687156
MIF	0.22312217	0.87289915	0.70143327	1.08627999
MMP10	0.75970906	1.02645461	0.86831007	1.21340186
COL4A2	0.33959936	1.10632847	0.89911642	1.36129498
MSX1	0.2684191	0.87684817	0.69477561	1.10663458
AGT	0.02241397	1.16207223	1.02149696	1.32199304
TM6SF2	0.72721607	0.9638293	0.78361411	1.18549029
ADAMTSL2	0.30475322	1.11331202	0.90696449	1.3666066
NOS3	0.25175718	1.18769131	0.8850155	1.59388242
OXTR	0.03034988	1.48851165	1.03847523	2.13357707

Table S2 (*continued*)

https://dx.doi.org/10.21037/jgo-22-872

Table S2 (*continued*)

Gene	P value	HR	Low 95% CI	High 95% CI
GDPD2	0.41534188	1.12008128	0.85259473	1.47148702
COMP	0.00400106	1.16217071	1.04911058	1.28741505
TNNC1	0.49237205	1.05731598	0.90178705	1.2396686
PLS3	0.12594973	1.27242598	0.93458682	1.73238896
ENG	0.1282404	1.22179058	0.94383971	1.58159506
CYB5A	0.17522309	0.77861208	0.54223989	1.11802319
TBX10	0.88747945	0.98106676	0.75284906	1.27846607
WNT5A	0.13497299	1.16690347	0.95309919	1.42866946
HES4	0.11921884	1.16339139	0.96171405	1.4073617
EMP1	0.24858925	1.11636108	0.92597122	1.34589718
NKD2	0.40623078	0.93756675	0.80525139	1.09162357
ICAM3	0.33670332	1.15228201	0.86291909	1.53867708
ADAMTS9	0.52613794	1.10024334	0.81886376	1.47831113
GATA5	0.00629847	1.17607841	1.0468907	1.32120806
RBKS	0.52761679	0.84276622	0.49565678	1.43295708
SLC28A2	0.34700519	1.0590472	0.93969747	1.19355539
PSD4	0.79836588	1.04262999	0.7568874	1.43624705
TESK2	0.38334046	0.8262369	0.53793738	1.26904626
DPYSL2	0.87572908	1.02061674	0.79029198	1.31806795
HIST3H2A	0.35262419	0.92439252	0.78317966	1.09106706
ADH4	0.11715351	1.11259696	0.97358414	1.27145866
LRRC32	0.0111805	1.27896772	1.05756049	1.546728
TM4SF18	0.43205563	0.87390282	0.62436188	1.22317866
FSTL3	0.05577273	1.16727347	0.99619414	1.36773275
BMPR2	0.02754286	1.52028288	1.04742781	2.20660557
CDH5	0.68685839	1.05284347	0.81965643	1.35237075
LUM	0.14615021	1.1192659	0.96147678	1.30294999
ACE2	0.33202725	1.07855791	0.92572759	1.2566193
CAT	0.54060353	0.90870262	0.6687189	1.23480951
MCOLN2	0.6794693	0.92920896	0.65593156	1.31634052
CREB3L3	0.10766477	1.11577128	0.97637053	1.2750749
TGFBI	0.63530008	0.95998672	0.81091668	1.13646016
IGFBP7	0.04813965	1.21907338	1.00162218	1.48373301
SH3PXD2B	0.27745434	1.14247435	0.89836563	1.4529136

Table S2 (*continued*)

https://dx.doi.org/10.21037/jgo-22-872

Table S2 (*continued*)

Gene	P value	HR	Low 95% CI	High 95% CI
SULT1B1	0.92713428	0.99335242	0.86103904	1.14599801
GJA4	0.18643645	1.1810521	0.92269775	1.51174539
TMEM147	0.49025722	0.8907499	0.64123168	1.2373615
UBTD1	0.12467599	1.26545518	0.93698011	1.70908304
SRPX2	0.02560073	1.28606148	1.03116003	1.60397423
COL15A1	0.83609672	1.01914003	0.85158941	1.21965633
KCNJ2	0.00227992	0.56969165	0.39688875	0.81773186
CLC	0.51502974	0.92948388	0.74581571	1.15838306
TMEM37	1.66E-05	1.45694392	1.22761785	1.72910941
INHBB	0.9192167	1.00755374	0.87118316	1.16527107
NNMT	0.00599303	1.26427618	1.06957	1.49442698
DDAH2	0.45743006	1.09202212	0.86574917	1.37743394
CLEC11A	0.12792356	1.1641382	0.95725113	1.41573898
POU2AF1	0.3765287	1.0760477	0.9147047	1.26584968
PTGER4	0.37792999	0.90774036	0.73200626	1.12566328
IFITM2	0.76375894	0.9714744	0.80439166	1.17326242
BRSK1	0.02340012	1.48236231	1.05473417	2.08336668
FSTL1	0.1923852	1.13508419	0.93818931	1.37330079
ITGBL1	0.1915254	1.13662299	0.93789849	1.37745378
LDB2	0.09855331	1.30462199	0.95162061	1.78856838
SLC4A2	0.24589488	0.821566	0.58947759	1.14503199
YAP1	0.35212766	0.86040435	0.62684279	1.18099091
PLVAP	0.21166549	1.16640424	0.91611001	1.48508239
CTSK	0.23537262	1.11429035	0.93190371	1.33237263
CALCRL	0.7580227	1.03797552	0.81885369	1.31573345
THBS1	0.07713538	1.14138423	0.98570778	1.32164723
PCDH18	0.34052356	1.13470399	0.87503458	1.47143117
LAMC1	0.07675353	1.22631439	0.97832261	1.53716879
EDNRA	0.17706792	1.15631101	0.9364623	1.42777254
PCOLCE	0.26638011	1.11102229	0.92276893	1.33768106
SLC6A8	0.75788287	0.97546576	0.83295389	1.1423603
PLEKHA4	0.00150854	1.39452068	1.13557173	1.7125188
TMEM119	0.01621229	1.23541716	1.03982866	1.46779524
FCER2	0.01272939	1.23551191	1.0461342	1.45917195

Table S2 (*continued*)

https://dx.doi.org/10.21037/jgo-22-872

Table S2 (*continued*)

Gene	P value	HR	Low 95% CI	High 95% CI
SLC7A9	0.98807551	0.99864621	0.83609788	1.19279605
CHP2	0.31773205	0.93292272	0.81412813	1.06905137
GLRX	0.72395889	0.94943652	0.7118871	1.26625375
GREM1	0.09947906	1.09998175	0.9820812	1.23203646
PTP4A3	0.34172254	0.90775414	0.74356965	1.10819153
NOTUM	0.6895214	0.9832378	0.90498545	1.06825647
MGP	0.05248828	1.11495664	0.99883028	1.24458413
AEBP1	0.02646637	1.18325482	1.01985759	1.37283085

https://dx.doi.org/10.21037/jgo-22-872